Proteomic Comparison of Prostate Cancer Cell Lines LNCaP-FGC and LNCaP-r Reveals Heatshock Protein 60 as a Marker for Prostate Malignancy

Björn Johansson,[1]* Mohammad R. Pourian,[2] Yin-Choy Chuan,[3] Irene Byman,[4] Anders Bergh,[5] See-Tong Pang,[2,3,6] Gunnar Norstedt,[3] Tomas Bergman,[4] and Åke Pousette[2]

[1]*Department of Clinical Neuroscience, Karolinska Hospital, Karolinska Institutet, Stockholm, Sweden*
[2]*Andrology Center, Department of Medicine, Karolinska Hospital, Karolinska Institutet, Stockholm, Sweden*
[3]*Department of Molecular Medicine, Karolinska Hospital, Karolinska Institutet, Stockholm, Sweden*
[4]*Department of Medical Biochemistry and Biophysics, Karolinska Institutet, Stockholm, Sweden*
[5]*Department of Pathology, Norrlands Universitetssjukhus, Umeå, Sweden*
[6]*Division of Urology, Department of Surgery, Chang Gung Memorial Hospital, Chang Gung University College of Medicine, Tao Yuan, Taiwan*

BACKGROUND. Androgen-sensitive prostate cancer cell-line LNCaP-FGC and androgen-resistant line LNCaP-r constitute a model for development of androgen resistance in prostate cancer.

METHODS. Proteins differently expressed in the two cell-lines were identified by two-dimensional (2-D) electrophoresis and mass spectrometry. HSP60, more abundant in LNCaP-r, was studied by RT-PCR and immunohistochemistry in specimens of human prostate cancer.

RESULTS. HSP60 was upregulated in LNCaP-r, nm23 in LNCaP-FGC, and titin (two isoforms) in either LNCaP-r or LNCaP-FGC. In non-malignant prostate, HSP60-staining was in the glandular compartment, particularly basal epithelial cells. In prostate cancer, most epithelial cells showed moderate-strong staining without apparent correlation between staining intensity and Gleason grade.

CONCLUSIONS. The LNCaP-FGC/LNCaP-r model, characterized by 2-D electrophoresis, reveals distinct proteomic alterations. With HSP60, results from cell-lines correlated with clinical results, indicating that this model can be used for dissection of mechanisms involved in transformation to androgen resistance and assignment of protein markers in prostate cancer. *Prostate 66: 1235–1244, 2006.*

KEY WORDS: **androgen resistance; immunohistochemistry; two-dimensional gel electrophoresis; mass spectrometry**

INTRODUCTION

Prostate cancer is the dominating cancer among men in industrialized Western countries [1]. In the United States, it has been estimated that one in every six men will be diagnosed with prostate cancer during their lifetime [2]. However, the molecular mechanisms in prostate cancer development and progression still remain largely unknown [3]. Prostate cancer is a heterogeneous disease with clinical phenotypes of varying aggressiveness. Organ-confined prostate cancer can be cured with radical prostatectomy, whereas

Grant sponsor: Swedish Cancer Foundation; Grant sponsor: Swedish Cancer Society; Grant sponsor: Swedish Research Council; Grant sponsor: Wallenberg Consortium North (Protein Analysis Center); Grant sponsor: Karolinska Institutet.

*Correspondence to: Dr. Björn Johansson, Department of Clinical Neuroscience, Karolinska Institutet, Karolinska Hospital CMM L8:01, SE-171 76 Stockholm, Sweden.
E-mail: Bjorn.Johansson@neuro.ki.se

Received 21 November 2005; Accepted 16 March 2006
DOI 10.1002/pros.20453
Published online 16 May 2006 in Wiley InterScience (www.interscience.wiley.com).

for patients with advanced tumors the prognosis is generally poor. Androgen ablation therapy remains the most commonly used palliative treatment for advanced prostate cancer and thus far there is no other effective route for treatment of the cancer [4]. The majority of patients will sooner or later develop androgen-resistant prostate cancer (ARPC), thus leading to a mortal outcome of the disease.

Several mechanisms have been proposed to be involved in ARPC progression. It has been suggested that androgen ablation may put a selective pressure on the prostate cancer cells that will eventually promote the emergence of ARPC cells. These ARPC cells can then restore the signaling pathways mediated by the androgen receptor (AR), following either mutation or amplification of AR [4] or through transactivation of AR by other signaling molecules [5]. In addition, genomic instability has been documented to cause and promote the emergence of ARPC cells [6–8]. Cytogenetically, ARPC cells can either be very different, even within the same tumor, or have only few additional genomic alterations as compared to the primary tumors. The acquisition of these additional genetic alterations may render the ARPC cells a growth advantage, without the need for stimulation by androgens, as well as the ability to resist the detrimental effect of androgen ablation. However, most of the involved oncogenes and/or tumor suppressor genes within these altered genomic regions are yet to be identified.

LNCaP-FGC (fast growing colony) is an androgen-responsive human prostate cancer cell line that has been widely used for the study of androgen action in prostate cancer [9,10]. LNCaP-r is an ARPC cell line that was derived from LNCaP-FGC and characterized in our laboratory [11,12]. Although LNCaP-r retains many features of LNCaP-FGC such as expression of AR, prostate specific antigen (PSA) and prostatic acid phosphatase (PAP), it does not respond by proliferation when stimulated by androgen. Phenotypically, LNCaP-r has achieved a more aggressive behavior compared to LNCaP-FGC. Thus, the two cell lines clearly mimic the clinical situation and provide a potentially useful model system to study the underlying mechanisms involved in transformation of prostate cancer into the androgen resistant state [12,13].

In this study we have characterized these two cancer cell lines using two-dimensional (2-D) gel electrophoresis and identification by mass spectrometry (MS). Based on the gel separation results, we focused our studies on heatshock protein 60 (HSP60) which is present at higher concentration in LNCaP-r. The expression of HSP60 was characterized in selected specimens and tissue arrays of prostatic tissues (totally 89 samples) using immunohistochemistry and quantitative real time reverse transcriptase-polymerase chain reaction (RT-PCR). Further confirmation and validation of the candidate proteins in clinical prostate cancer will provide an opportunity to assign novel prognostic tumor markers and development of therapeutic strategies.

MATERIALS AND METHODS

Cell Cultures

LNCaP-FGC human prostate cancer cells were obtained from the American Type Culture Collection (ATCC), Rockville, MD. The derivative of LNCaP which is androgen insensitive, the LNCaP-r subline (passage 40), was developed in our laboratory and maintained as described [11]. Cells with a narrow range of passage numbers were used for all experiments (LNCaP-FGC, 23–28; LNCaP-r, 44–47).

For routine maintenance, cells were grown in RPMI-1640 medium containing 5 mg/ml phenol red and supplemented with 10% inactivated fetal bovine serum (FBS), 2 mM L-glutamine and antibiotics (50 mg/ml each of penicillin and streptomycin) (all purchased from Life Technologies Ltd, Paisley, UK or Invitrogen). Cells were harvested using a mixture of 0.05% trypsin and 0.01% EDTA, and subcultured at 1:4–1:6 ratio in 25 cm^2 culture flasks (Corning Costar Corp., Cambridge, MA) at 37°C in a humidified atmosphere of 5% CO_2 in air. Culture medium and cells were routinely tested for mycoplasma contamination.

Treatment With Hormones

After subculturing, cells were left undisturbed for 24–48 hr to allow attachment to the surface. To avoid interfering factors that might modify the metabolic ability of the cells, the medium was substituted with phenol red-free RPMI-1640 with 5% dextran coated charcoal treated FBS (DCC-FBS) (Hyclone Inc, Logan, UT) for 24 hr prior to exposure to the same medium containing 0.1% ethanol (control) and 10 nM androgen R1881. Cells were washed twice with PBS before harvested by scraping and transfer to sterile plastic tubes for storage at −80°C until use. For real-time RT-PCR, cells were treated with R1881 for 2 and 8 hr. To test whether the regulation of HSP-60 expression by androgen is a primary event, 10 μM of androgen antagonist Casodex (Astra-Zeneca, Sweden) and 10 μg of protein synthesis inhibitor cycloheximide (CHX) were separately added to the cells 2 hr and 30 min prior to hormone stimulation.

2-D Gel Electrophoresis

Samples of androgen sensitive and insensitive forms of epithelial prostate cancer cell lines (LNCaP-FGC and

LNCaP-r, respectively) were prepared for 2-D gel electrophoresis essentially as described [14]. Cells were resuspended in 25–30 μl water followed by freezing and thawing four times. Cells were then mixed with 0.3289 × w.w. DNase I (Worthington or ICN Biomedical Inc.) and 0.0888 × w.w. RNase A (ICN Biomedical Inc.), and incubated 5–10 min at 4°C. To the solution, 500 μl lysis buffer (9 M urea, 4% Chaps, 1.6 mM *Tris* base) was added and incubation was performed overnight at room temperature. Protein concentration was determined with the BCA protein assay reagent kit (Pierce). For subsequent detection by silver and colloidal Coomassie blue staining, 100 and 1,000 μg total protein was loaded, respectively, in 24 cm strip holders and immobiline drystrip gels (IPG strips, Amersham Pharmacia Biotech) were positioned and covered with 300 μl cover fluid.

The first dimension isoelectric focusing (IEF) was performed in the intervals pH 3–10 or 4–7 (linear, 24 cm strips) using a Pharmacia IPGphor system overnight. Following IEF, proteins were separated in the second dimension SDS–PAGE overnight. IPG strips were applied to pre-cast gels (12.5% acrylamide) in an Ettan DALT II system according to the manufacturers instruction (Amersham Pharmacia Biotech). Briefly, IPG strips were equilibrated in 1.5 M Tris-Cl (pH 8.8), 6 M urea, 87% glycerol and 14 mM SDS with a trace of bromophenol blue and 1% dithiothreitol (DTT) in individual tubes for 15 min. This was followed by 15 min incubation in the same buffer but without DTT and containing 2.5% iodoacetamide before transfer to SDS–PAGE.

Proteins were detected by staining with colloidal Coomassie blue or silver. Gels were visually compared and selected spots were excised for identification by in-gel tryptic digestion and MS.

In-Gel Digestion

Protein spots were excised manually from the Coomassie-stained gels. Gel pieces were processed and digested with trypsin using a robotic protein handling system (MassPREP, Waters) employing a protocol based on in-gel digestion methods [15]. Gel pieces were destained twice in 100 μl 50 mM ammonium bicarbonate (Ambic)/acetonitrile (1:1, v/v) at 40°C for 10 min. Proteins were reduced by treatment in 10 mM DTT/100 mM Ambic for 30 min, gel pieces were shrunk in acetonitrile, and alkylation was carried out in 55 mM iodoacetamide/100 mM Ambic for 20 min. Trypsin (Promega modified, 25 μl of a 12 ng/μl solution in 50 mM Ambic) was added, and digestion was allowed to proceed for 4.5 hr at 40°C. Peptides were extracted with 30 μl 5% formic acid/2% acetonitrile followed by 24 μl 2.5% formic acid/50% acetonitrile.

Mass Spectrometry

Tryptic peptides were analyzed by matrix-assisted laser desorption/ionization (MALDI) MS in a Voyager DE-Pro instrument (Applied Biosystems). For peptides with m/z less than 4,000, the MALDI instrument was operated in reflectron mode, while larger peptides were analyzed in linear mode. Protein Prospector MS-Fit search tool was used for database searches of peptide mass fingerprint data.

Digests were desalted employing C_{18} ZipTips (Millipore). Before desalting, acetonitrile was evaporated from samples under a stream of nitrogen. The ZipTips were activated and equilibrated using 10 μl 70% acetonitrile/0.1% trifluoroacetic acid (TFA) twice, 10 μl 50% acetonitrile/0.1% TFA twice, and finally 10 μl 0.1% TFA twice. The samples were loaded onto ZipTips by pipetting 20 times and washed twice using 10 μl 0.1% TFA. The tryptic peptides were eluted with 60% acetonitrile/1% acetic acid.

HumanTissues

Paraffin embedded prostate cancer tissue sections of different Gleason grades and from one patient on androgen ablation therapy prior to radical prostatectomy were retrieved from the files at the Department of Pathology, Umeå University. Sections were selected from 9 patients with different Gleason scores.

Tissue microarray slides were obtained from the Cooperative Human Tissue Network and the Tissue Array Research Program (TARP) of the National Network and the Tissue Array Research Program (TARP) of the National Cancer Institutes of Health, Bethesda, MD, USA. These arrays (T-PR-1C) contain totally 79 prostatic samples and 72 matched controls including tumors with Gleason score 6–8 including primary Gleason grade 3–5.

Western Blotting

LNCaP cells were cultivated as described (above). The cells were harvested using RIPA (radioimmunoprecipitation) buffer with protease inhibitor. Protein concentration was determined with BCA protein assay reagent (Pierce). Equal amounts of protein were denatured with loading buffer, separated on 12% SDS–PAGE (Invitrogen) and blotted onto PVDF membrane (Amersham). Membranes were blocked in *Tris*-buffered saline (TBS) solution with 5% non-fat dry milk and probed with primary antibody. The membranes were washed in TBS-(Tween)T four times, 15 min each, and then incubated 1 hr with horseradish peroxidase (HRP) conjugated second antibody (Pierce), followed by washing four times, 15 min each, in TBS-T.

For detection, the ECL Western kit (Amersham) was used and the blot was placed on an autoradiography

film (Hyperfilm ECL, Amersham) to visualize the antigen-antibody HRP complex. Mouse monoclonal anti-human HSP60 antibody (1:500 dilution) was obtained from Santa Cruz Biotechnology (Santa Cruz, CA). Mouse anti-human beta-actin antibody (1:50,000 dilution) was obtained from Sigma.

Immunohistochemistry

Paraffin sections (4 μm) from tumors and tissue microarrays were deparaffinated and dehydrated according to standard procedures. The primary antibody, mouse monoclonal anti-human HSP60 antibody (HSP60, sc-13115) was obtained from Santa Cruz Biotechnology (Santa Cruz, CA) and diluted 1:100 in 3% PBS, and the slides were incubated for 1.5 hr at room temperature. The slides were washed three times for 5 min each in phosphate-buffered saline (PBS) before 45–60 min incubation with the secondary anti-mouse IgG antibody (DAKO A/S, F0205). Control slides were incubated with secondary antibody only. After washing three times, 5 min each, in PBS, the slides were mounted (mounting medium was 0.5 g diazabicyclooctane (Sigma) in a solution of 0.5 ml PBS and 4.5 ml glycerol, pH 8.5–8.9). The slides were evaluated using a Zeiss Axioskop and 20 times magnification.

Quantitative Real-Time Reverse Transcriptase-Polymerase Chain Reaction

Total RNA was extracted using TRIzol (Life Technologies, Inc., manufacturers protocol). The concentration of total RNA was measured by OD-readings and quality was checked on BioAnalyzer (Agilent Technologies Deutschland GmbH, Waldbronn, Germany). Total RNA (5 μg) from different samples was first treated with RQ1 DNase (Promega, manufacturers protocol). It was then reverse-transcribed using Superscript II (Life Technologies Inc.) in a reaction volume of 20 μl. After the reverse transcription, the volume was brought up to 60 μl with diethyl pyrocarbonate (DEPC)-treated water. The synthesized cDNAs were used to measure the expression of HSP60 using DNA Engine Opticon 2 (MJ Research, Inc.). The real-time PCR reactions were performed in 20 μl with 2 μl of the respective cDNA sample and 0.4 μM primers. SYBR Green I dye, hot-start iTaq DNA polymerase, optimized buffer, and dNTPs qualified for quantitative PCR were supplied in the iQ SYBR Green supermix (BioRad). The amplification program consisted of 1 cycle at 95°C for 10 min (hot start) followed by 45 cycles at 95°C for 10 sec, annealing temperature was 58°C for 10 sec and 72°C for 15 sec. Fluorescence intensity was measured at a specific acquisition temperature for each gene. For each studied gene, a relative standard curve was constructed with serial dilution (1:1, 1:10, 1:100 for beta actin, and 1:1, 1:5 and 1:10 for HSP60) using a pool of all cDNA samples. The relative concentration of gene expression in unknown samples was calculated using Opticon Monitor software and measurements were performed in triplicate for each sample. The level of individual mRNA measured was normalized to the internal control gene beta actin. The primers used were: Beta actin, 5′-CTG GCT GCT GAC CGA GG-3′ (forward) and 5′-GAA GGT CTC AAA CAT GAT CTG GGT-3′ (reverse); HSP60, 5′-ATT CCA GCA ATG ACC ATT GC-3′ (forward) and 5′-GAG TTA GAA CAT GCC ACC TC-3′ (reverse).

To validate the real-time PCR procedure, the expression pattern of a known androgen-responsive gene, STE20, coding for a protein kinase, was also included in the analysis [16].

RESULTS

2-D Gel Electrophoresis and Identification of Proteins by Mass Spectrometry

Using cell culture conditions and 2-D gel electrophoresis as specified, reproducible protein patterns were obtained for both LNCaP-FGC and LNCaP-r preparations (Fig. 1). Visual comparison of the gels revealed a number of spots for which the staining was significantly more intense in either of the cell line separations. There were approximately 120 visible and distinct protein spots on each (LNCaP-FGC and LNCaP-r) gel. Twelve of the LNCaP-FGC protein spots were weaker (or absent) in LNCaP-r, and nine of the LNCaP-r protein spots were weaker (or absent) in LNCaP-FGC. Table I contains a list of 10 of these spots that were selected for analysis by MS after in-gel digestion of the corresponding protein components [17].

In several spots, more than one protein was identified and some proteins were found in more than a single spot. The latter indicates proteolytic processing and the occurrence of protein variants with charge differences corresponding to structural modifications such as deamidation (native or artificial) and phosphorylation [19]. Essentially all of the proteins identified in spots 4–10 (Table I) correspond to degradation products of large parent molecules with sizes exceeding the separation range of the gel which is approximately 100–10 kDa. The polypeptides identified in these spots thus represent cleavage products of larger precursors, and it is difficult at this stage to tell if the reason is native processing or proteolytic activity during the sample preparation steps. Nevertheless, the presence of these polypeptides and their staining are indicators of their expression and relative abundance in the cell line investigated (see also Discussion). The proteins identified in spots 1–3 do not reveal the

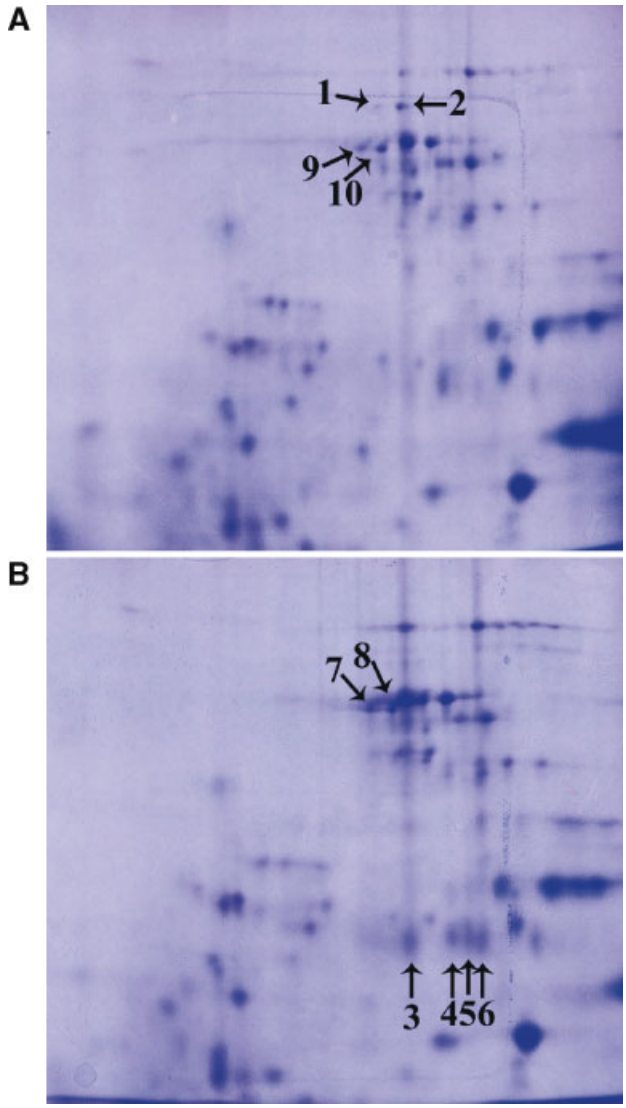

Fig. 1. 2-D gel separation of LNCaP-r (**A**) and LNCaP-FGC (**B**) proteins. Isoelectric focusing was carried out in the pH-range 4–7 (linear). Staining was by Coomassie blue. Spot numbers refer to Table I. [Color figure can be viewed in the online issue, which is available at www.interscience.wiley.com.]

same type of extensive processing and are more of a size directly comparable to that of the parent molecule (Table I and Fig. 1).

HSP60 [20] was identified in both spots 1 and 2 at solid MOWSE scores of the order 10^5–10^6. The components of spots 1 and 2 are of the same size but they differ in their isoelectric location (Fig. 1), indicating the presence of charge isoforms of HSP60. Interestingly, spots 1 and 2 are hardly visible in the LNCaP-FGC cell line preparation. HSP60 expression is thus clearly predominant in the LNCaP-r cell line.

Analysis of spot 3 revealed two nucleoside diphosphate kinases, enzymes involved in the synthesis of nucleoside triphosphates. They are nucleoside diphosphate kinase B (nm23 variant H2) and a putative nucleoside diphosphate kinase, both identified at MOWSE scores exceeding 1,000.

Polypeptide segments of two isoforms of the giant protein titin, a component of vertebrate striated muscle important for ultrastructure and elasticity [21], were identified in spots 4, 6–8, and 10. The MOWSE scores were between 3,000 and 180,000, and the number of matching tryptic peptides were between 14 and 21 (Table I). The two titin isoforms detected, N2-A and N2-B, derive from the same gene through alternative splicing. Along with titin, the structural protein collagen was detected in spot 6 and a human coronavirus replicase polyprotein in spot 8.

Spot 5 revealed three protein components, the muscle protein myosin (variant 5C), the membrane-cytoskeleton linker protein ankyrin 3, and DNA (cytosine-5)-methyltransferase 3A (Dnmt3a). All three proteins were identified at fairly low MOWSE scores, between 200 and 600 (Table I). However, the number of matching peptides was four and above, which can be considered reasonably safe.

Spot 9 was found to contain one major component, the colonic and hepatic tumor over-expressed protein (CH-TOG). This protein plays an important role in the organization of spindle poles [22] and, as the name suggests, the cellular levels are significantly increased in hepatomas and colonic tumors [23].

Based on the protein identification results (Table I), HSP60 was selected for further studies since this protein was one of the major proteins upregulated in LNCaP-r cells compared to those of LNCaP-FGC, and did furthermore show a high MOWSE score for identification.

Western Blot and Immunohistochemistry of HSP60

Western blots of cell extracts from LNCaP-FGC and LNCaP-r showed one band corresponding to 60 kDa where the band from LNCaP-r was much stronger (Fig. 2A). The elevated level of HSP60 in LNCaP-r compared to that in LNCaP-FGC was confirmed by RT-PCR measurements (Fig. 2B and below). Using immunohistochemistry, HSP60-staining was observed in the glandular compartment in non-malignant prostate tissue, particularly in basal epithelial cells (Fig. 3). In prostate cancer, most epithelial cells showed moderate to strong HSP60 staining (Fig. 4). There was no apparent relation between Gleason grade and staining intensity (Figs. 4 and 5). In prostate tissue from an androgen-ablated patient, some of the tumor cells were stained for HSP60 whereas others were largely unstained (Fig. 6). A similar pattern was also seen for the tissue array samples.

TABLE I. Proteins Identified in LNCaP-FGC/LNCaP-R Cell Lines After 2-D Gel Electrophoresis (Fig. 1), In-Gel Digestion and Peptide Mass Fingerprinting

Spot no. (Fig. 1)	Cell line with pre-dominant expression	MOWSE score[a]	No. of peptides matched (% of total)	Sequence coverage (%)	Accession number	Molecular size (kDa)	Protein
1	LNCaP-r	8.1×10^6	10 (59)	24	P10809	61.1	60 kDa heat shock protein (HSP60)
2	LNCaP-r	1.1×10^5	9 (30)	22	P10809	61.1	60 kDa heat shock protein (HSP60)
3	LNCaP-FGC	1,446	4 (21)	26	O60361	15.5	Putative nucleoside diphosphate kinase (NDK)
		1,298	4 (21)	23	P22392	17.3	Nucleoside diphosphate kinase B (nm23-H2; C-myc purine-binding transcription factor PUF)
4	LNCaP-r	42,570	20 (67)	1	19747267	3713.8	Titin (isoform N2-A)[b]
5	LNCaP-FGC	563	7 (27)	4	Q9NQX4	202.8	Myosin Vc (Myosin 5C)
		359	7 (27)	2	Q12955	480.4	Ankyrin 3 (ANK-3) (Ankyrin G)
		218	4 (15)	6	Q9Y6K1	101.6	DNA (cytosine-5)-methyltransferase 3A (Dnmt3a)
6	LNCaP-FGC	3,059	21 (84)	1	20143914	2993.0	Titin (isoform N2-B)[b]
		2,399	8 (32)	2	P12111	343.6	Collagen alpha 3(VI) chain precursor
7	LNCaP-FGC	1.8×10^5	19 (46)	1	20143914	2993.0	Titin (isoform N2-B)[b]
8	LNCaP-FGC	5,305	14 (58)	1	17066105	3816	Titin (isoform N2-B)[b]
		3,231	9 (38)	2	49169783	752.7	Replicase polyprotein 1ab (Human coronavirus NL63)
9	LNCaP-r	632	5 (29)	3	Q14008	225.5	CH-TOG protein (Colonic and hepatic tumor overexpressed protein)
10	LNCaP-r	7,727	16 (59)	1	1212992	2993.5	Titin (isoform N2-B)[b]

Accession number given is for SwissProt or GenBank.
[a]The principles for MOWSE scoring are described in Pappin et al. [18]. Mass tolerance applied in the database searches was 0.1 Da. The cell line preparation (LNCaP-FGC or LNCaP-r) that showed the most intense gel spot was normally used for protein identification.
[b]Two isoforms of titin matched the data for several gel spots. However, both isoforms derive from the same gene through alternative splicing.

Real-Time Quantitative PCR for HSP60

RT-PCR showed that HSP60 mRNA level was significantly higher in LNCaP-r compared to that in LNCaP-FGC ($P < 0.05$; Student's t-test; Fig. 2B). The results from one ablated patient indicated that HSP60 may be androgen sensitive and therefore quantitative RT-PCR of HSP60 was performed on LNCaP-FGC cells with and without androgen stimulation. Androgen treatment of the LNCaP-FGC cell line indicated that there was no clear androgen influence on HSP60 mRNA levels (Control $100 \pm 53\%$; R1881, 2 hr $122 \pm 54\%$; R1881, 8 hr, $144 \pm 46\%$; R1881, 20 h, $99 \pm 22\%$). These differences are not statistically significant ($P > 0.05$, Student's t-test). The known androgen-sensitive gene STE20 (see Materials and Methods) was strongly upregulated at the same time-points, confirming the sensitivity of our RT-PCR procedure.

DISCUSSION

Application of 2-D gel electrophoresis to LNCaP-FGC and LNCaP-r cell lines generated reproducible protein patterns and selected spots could be tentatively identified (Fig. 1 and Table I). Selection of spots by visual inspection implicates that only proteins present at high concentration and differing substantially in expression between the two cell lines will be studied. Despite this fact, the results show that 2-D gel electrophoresis combined with MS is a useful approach to partial comparison of the protein expression patterns in the two prostatic cancer cell lines.

However, several spots that were found to be different between LNCaP-FGC and LNCaP-r are representing cleavage products of larger protein molecules. One example is titin (Table I) that was present in a number of spots in both separations, but since the molecular weight of this muscle protein is 3–4 MDa [21], these spots represent cleavage products that probably were formed during tissue preparation. Consequently, it is possible that some of the differences detected are due to causes such as different proteolytic activity in the two cell lines. A further complication at this stage is when two or more proteins are detected in a single spot. In such cases it is not possible to safely

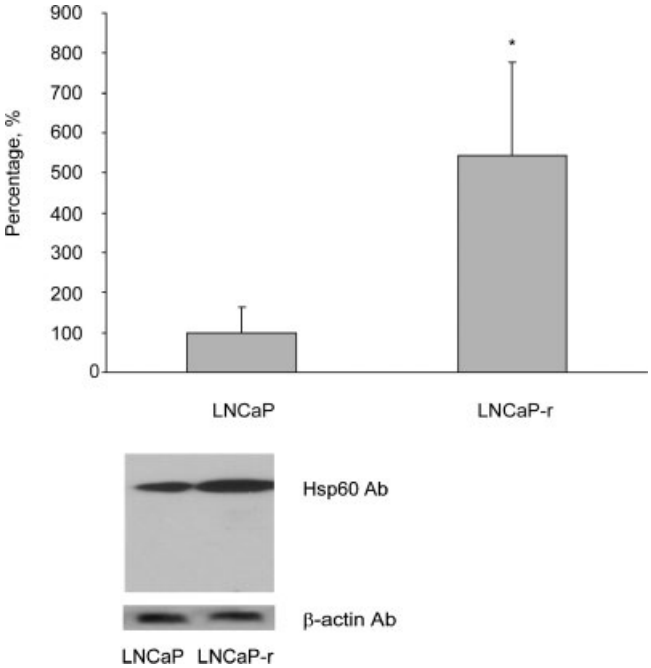

Fig. 2. **A**: HSP60 immunoblot. The results are representative of three experiments each. **B**: Quantitative RT-PCR measurements of HSP60 expression in LNCaP-FGC ("LNCaP" in this figure) and LNCaP-r cell lines. Each column represents the average of three measurements and error bars represent S.E.M. Values for the control sample were set to 100%. The asterisk indicates a statistically significant difference to the control (LNCaP-FGC; $P < 0.05$; Student's *t*-test).

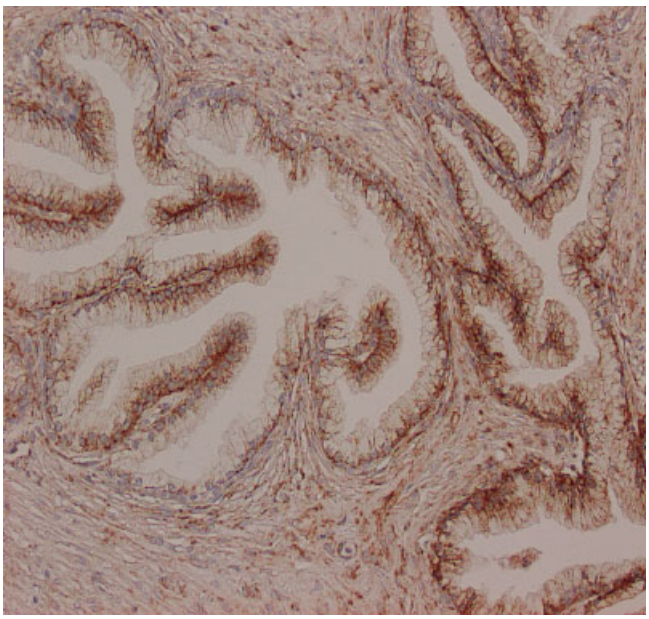

Fig. 3. Immunolocalization of HSP60 in a non-malignant prostate tissue section. HSP60 staining is observed in the glandular compartment, particularly in basal epithelial cells. [Color figure can be viewed in the online issue, which is available at www.interscience.wiley.com.]

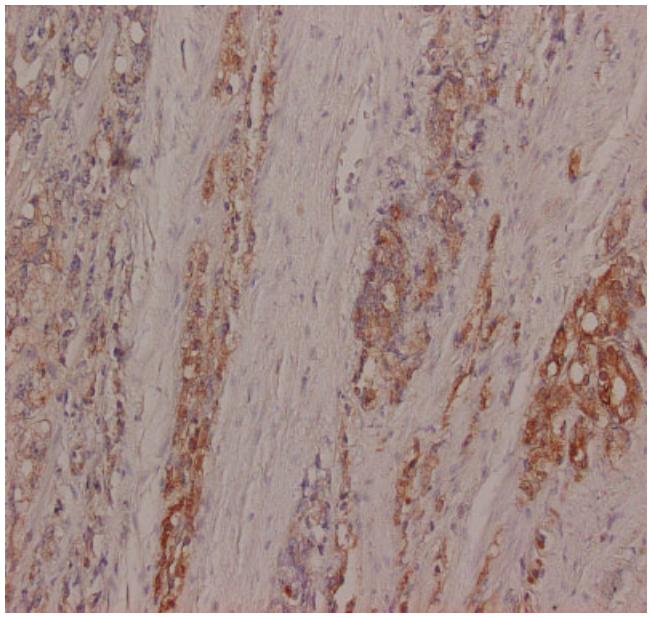

Fig. 4. Immunolocalization of HSP60 in a malignant prostate tissue section. In this Gleason grade 3 prostate cancers, most epithelial cells show moderate to strong HSP60 staining. [Color figure can be viewed in the online issue, which is available at www.interscience.wiley.com.]

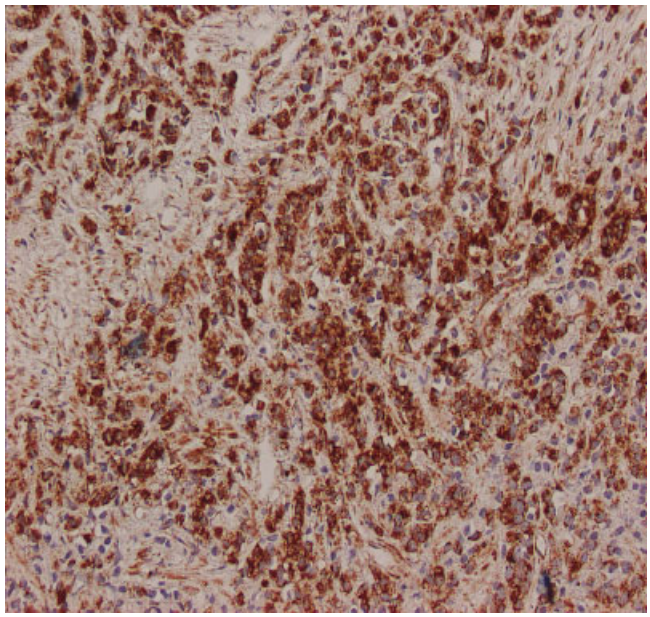

Fig. 5. Immunolocalization of HSP60 in a malignant prostate tissue section. In this Gleason grade 5 prostate cancer, most epithelial cells show moderate to strong HSP60 staining. There is no apparent relation between staining intensity and Gleason grade. [Color figure can be viewed in the online issue, which is available at www.interscience.wiley.com.]

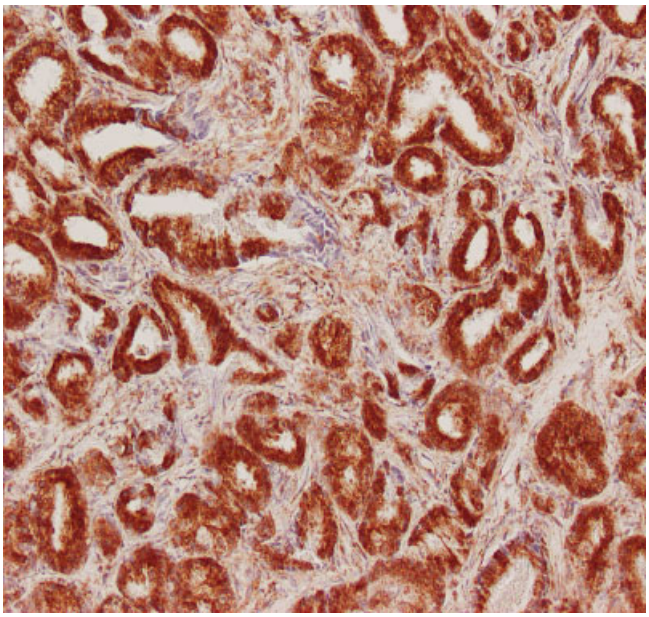

Fig. 6. Immunolocalization of HSP60 in a prostate tissue section after androgen ablation therapy. Some tumor cells are stained for HSP60, whereas others are largely unstained. [Color figure can be viewed in the online issue, which is available at www.interscience.wiley.com.]

judge the contribution of each component to the staining (MS analysis without specific labeling is not quantitative) and thus not possible to make assignments of the relative abundance of each of the proteins found in a particular spot. Nevertheless, the mere presence of a protein in a multiple-component spot is still an indicator of its expression.

In order to compare the data with clinical cases, we decided to select one protein for a more careful study. A significant finding was the higher concentration of HSP60 in the LNCaP-r cell line and since this protein was identified at a high score and the literature concerning HSP60 and prostate tissue is scanty, we chose this protein for a thorough investigation. In recent years, the biological role of heatshock proteins has been partly revealed [24]. The heatshock proteins can act as molecular chaperones that bind to unfolded or unassembled polypeptides aiding in protein biogenesis according to two general principles: they block non-productive protein–protein interactions and they mediate the folding of proteins to their native state. The HSP60 is present in many different organisms and tissues, and is abundant in most mammalian cells under normal conditions [24]. Aberrant expression of HSP60 has been associated with autoimmune diseases and is thought to have a role in antigen presentation in malignant diseases [25]. The biological role of HSP60 and its possible use as a marker in carcinogenesis has been explored in a few cases. It has also been shown that HSP60, as well as HSP70 and HSP90, are capable of inducing the production of proinflammatory cytokines by the monocyte-macrophage system [26].

In a few studies, HSP60 has been investigated in relation to prostate tissue. In one study, the presence of HSPs 27, 60, and 70 was correlated to prostatic malignancy using immunohistochemistry [27]. It was found that heatshock protein expression independently can predict the clinical outcome in prostate cancer. HSP60 was significantly upregulated in both early and advanced prostate cancer when compared to normal prostatic epithelium. However, no consistent correlation was found between the levels of HSP60 and phenotypic behavior of individual primary prostatic cancers. In another study using similar methods, overexpression of HSP60 was found in early prostate carcinogenesis [28]. These results are in line with our findings for androgen sensitive/resistant prostate cancer, and as a consensus it seems likely that HSP60 in most cases is increased in prostatic cancer tissue but there is no clear correlation to the Gleason score. Previous and current results thus indicate that HSP60 expression may be useful as an independent marker for carcinogenesis.

Another interesting observation was that HSP60 is upregulated in LNCaP-r (Fig. 2), despite the presence of an AR incapable to mediate stimulation of proliferation. Since it is known that HSPs binds to and inactivates ARs, it is tempting to speculate that increased concentration of HSP60 blocks binding of androgens to the receptor. Studies are now in progress to knock out HSP60 in the LNCaP-r cell line using the siRNA technique to further investigate its biological role.

The protein nm23-H2 was identified in LNCaP-FGC (spot 3). This protein may have a role in the regulation of signal transduction by interaction with G-proteins, causing activation/inactivation of developmental pathways [29]. There are two human homologs described for the nm23 gene (H1 and H2) encoding heterodimeric protein products. The nm23-H2 protein variant (now identified in spot 3) has been shown to associate with human telomeres and also to increase the affinity of telomerase for its substrate which suggests a new biological role for nucleoside diphosphate kinases [30]. The nm23 gene has been identified in metastasis suppression where it halt metastasis in vivo without affecting primary tumor growth, a phenomenon suggested to involve diminished signal transduction downstream of a particular receptor and a histidine protein kinase activity [31].

Dnmt3a that was identified in LNCaP-FGC (spot 5) belongs to a group of proteins required for genome wide de novo methylation, essential for proper development. It might be of special interest in this study since it has been suggested to have a coordinating role in mRNA overexpression in tumors [32].

Altogether, our results suggest that the proposed model system (LNCaP-FGC/LNCaP-r) can be used to investigate at least some of the regulations involved in the development of prostate cancer. 2-D gel electrophoresis combined with MS is in this respect a useful first approach to get an overview of proteomic alterations in these cell lines. Findings of interest should then be verified and further explored using clinical material.

CONCLUSIONS

We have at the proteome level characterized an in vitro model for the development of ARPC. Unique proteins and dysregulated genes pointing towards potential candidates associated with the transformation to ARPC have been identified (Table I). The implications of these proteins for prostate cancer progression and their potential role as molecular markers now await further evaluation in clinical material.

ACKNOWLEDGMENTS

This study was supported by grants from the Swedish Cancer Foundation (ÅP), the Swedish Cancer Society (ÅP), the Swedish Research Council (GN, TB), the Wallenberg Consortium North (GN, TB and Protein Analysis Center) and Karolinska Institutet (BJ, ÅP, GN, TB).

REFERENCES

1. Mettlin C. Recent developments in the epidemiology of prostate cancer. Eur J Cancer 1997;33(3):340–347.
2. Scardino PT, Weaver R, Hudson MA. Early detection of prostate cancer. Hum Pathol 1992;23(3):211–222.
3. Grönberg H. Prostate cancer epidemiology. Lancet 2003;361 (9360):859–864.
4. Reid P, Kantoff P, Oh W. Antiandrogens in prostate cancer. Invest New Drugs 1999;17(3):271–284.
5. Parczyk K. Schneider MR. The future of antihormone therapy: Innovations based on an established principle. J Cancer Res Clin Oncol 1996;122(7):383–396.
6. Cher ML, Bova GS, Moore DH, Small EJ, Carroll PR, Pin SS, Epstein JI, Isaacs WB, Jensen RH. Genetic alterations in untreated metastases and androgen-independent prostate cancer detected by comparative genomic hybridization and allelotyping. Cancer Res 1996;56(13):3091–3102.
7. Nupponen NN, Hyytinen ER, Kallioniemi AH, Visakorpi T. Genetic alterations in prostate cancer cell lines detected by comparative genomic hybridization. Cancer Genet Cytogenet 1998;101:53–57.
8. Nupponen NN. Visakorpi T. Molecular cytogenetics of prostate cancer. Microsc Res Tech 2000;51(5):456–463.
9. Horoszewicz JS, Leong SS, Kawinski E, Karr JP, Rosenthal H, Chu TM, Mirand EA, Murphy GP. LNCaP model of human prostatic carcinoma. Cancer Res 1983;43(4):1809–1818.
10. Horoszewicz JS, Leong SS, Chu TM, Wajsman ZL, Friedman M, Papsidero L, Kim U, Chai LS, Kakati S, Arya SK, Sandberg AA. The LNCaP cell line—a new model for studies on human prostatic carcinoma. Prog Clin Biol Res 1980;37:115–132.
11. Hasenson M, Hartley-Asp B, Kihlfors C, Lundin A, Gustafsson JA, Pousette A. Effect of hormones on growth and ATP content of a human prostatic carcinoma cell line, LNCaP-r. Prostate 1985;7(2):183–194.
12. Pousette A, Carlstrom K, Henriksson P, Grande M, Stege R. Use of a hormone-sensitive (LNCaP) and a hormone-resistant (LNCaP-r) cell line in prostate cancer research. Prostate 1997; 31(3):198–203.
13. Zhao X, van Steenbrugge GJ, Schröder FH. Differential sensitivity of hormone-responsive and unresponsive human prostate cancer cells (LNCaP) to tumor necrosis factor. Urol Res 1992: 20(3):193–197.
14. Berkelman T, Stenstedt T. 2-D Electrophoresis using immobilized pH gradients. Pisentaway NJ: Amersham Pharmacia Biotech Inc. 1998.
15. Oppermann M, Cols N, Nyman T, Helin J, Saarinen J, Byman I, Toran N, Alaiya AA, Bergman T, Kalkkinen N, Gonzalez-Duarte R, Jörnvall H. Identification of foetal brain proteins by two-dimensional gel electrophoresis and mass spectrometry comparison of samples from individuals with or without chromosome 21 trisomy. Eur J Biochem 2000;267(15):4713–4719.
16. Qi H, Labrie Y, Grenier J, Fournier A, Fillion C, Labrie C. Androgens induce expression of SPAK, a STE20/SPS1-related kinase, in LNCaP human prostate cancer cells. Mol Cell Endocrinol 2001;182(2):181–192.
17. Jollès P, Jörnvall H, editors. Proteomics in functional genomics. Basel-Boston-Berlin: Birkhäuser, 2000.
18. Pappin DJC, Hojrup P, Bleasby AJ. Rapid identification of proteins by peptide-mass fingerprinting. Current Biol 1993;3(6):327–332.
19. Meri S, Baumann M. Proteomics: Posttranslational modifications, immune responses and current analytical tools. Biomol Eng 2001;18(5):213–220.
20. Cheng MY, Hartl FU, Horwich AL. The mitochondrial chaperonin hsp60 is required for its own assembly. Nature 2000; 348(6300):455–458.
21. Labeit S, Kolmerer B. Titins: Giant proteins in charge of muscle ultrastructure and elasticity. Science 1995;270(5234):293–296.
22. Gergely F, Draviam VM, Raff JW. The ch-TOG/XMAP215 protein is essential for spindle pole organization in human somatic cells. Genes Dev 2003;17(3):336–341.
23. Charrasse S, Mazel M, Taviaux S, Berta P, Chow T, Larroque C. Characterization of the cDNA and pattern of expression of a new gene over-expressed in human hepatomas and colonic tumors. Eur J Biochem 1995;234(2):406–413.
24. Christians ES, Zhou Q, Renard J, Benjamin IJ. Heat shock proteins in mammalian development. Semin Cell Dev Biol. 2003;14(5):283–290.
25. Multhoff G. Activation of natural killer cells by heat shock protein 70. Int J Hyperthermia 2002;18(6):576–585.
26. van Eden W, van der Zee R, Prakken B. Heat-shock proteins induce T-cell regulation of chronic inflammation. Nat Rev Immunol. 2005;5(4):318–330.
27. Cornford PA, Dodson AR, Parsons KF, Desmond AD, Woolfenden A, Fordham M, Neoptolemos JP, Ke Y, Foster CS. Heat shock protein expression independently predicts clinical outcome in prostate cancer. Cancer Res 2000;60(24):7099–7105.

28. Cappello F, Rappa F, David S, Anzalone R, Zummo G. Immunohistochemical evaluation of PCNA, p53, HSP60, HSP10 and MUC-2 presence and expression in prostate carcinogenesis. Anticancer Res 2003;23(2B):1325–1331.
29. Lee CS, Clarke RA, Tran KT, Kearsly JH, Chou ST. nm23 protein expression and p53 immunoreactivity in cutaneous fibrohistocytic tumors. Pathology 1999;31(2):123–126.
30. Nosaka K, Kawahara M, Masuda M, Satomi Y, Nishino H. Association of nucleoside diphosphate kinase nm23-H2 with human telomeres. Biochem Biophys Res Commun 1998; 243(2): 342–348.
31. Ouatas T, Salerno M, Palmieri D, Steeg PS. Basic and translational advances in cancer metastasis: nm 23. J Bioener Biomemb 2003;35(1):73–79.
32. Robertson KD, Uzvolgyi E, Liang G, Talmadge C, Sumegi J, Gonzales FA, Jones PA. The human DNA methyltransferases (DNMTs) 1, 3a and 3b: Coordinate mRNA expression in normal tissues and overexpression in tumors. Nucl Acids Res 1999; 27(11):2291–2298.